Embedded Barometric Pressure Sensor Unit
for Force Myography in Exoskeletons

Charlotte Marquardt, Pascal Weiner, Miha Dežman, and Tamim Asfour

Abstract— **Exoskeletons and other wearable devices benefit from sensor systems that are based on biofeedback for detecting muscle activity. However, such sensor systems in wearable applications are often impractical due to the need for direct skin contact or due to non-linear signal output, both requiring extensive calibration and post-processing. This paper presents a compact and robust barometer-based pressure sensor unit for detecting surface muscle pressure in an exoskeleton interface shell that is light, thin and does not require direct contact with the skin. It consists of an array of five miniature barometric sensors mounted on a custom embedded printed circuit board enclosed in a silicon dome. Evaluation of this sensor unit in a controlled experimental setup showed high sensitivity and an almost linear response to the normal force applied to the silicon dome. Additionally, a pilot study was conducted with four participants in a wearable application to compare the performance of the proposed sensor with that of electromyography (EMG). The results showed higher robustness to positioning, consistent signal, low variance and inter-subject variability compared to EMG.**

I. INTRODUCTION

Wearable robots, such as exoskeletons, interact closely with human users in both physical and cognitive terms. In order to provide assistance during activities of daily living at exactly the right instance during the motion, user intention recognition is required [1]. Measuring muscle activation and interaction forces provides valuable information to recognize the intention of the human regarding the general motion that is planned, but also which specific joint will be in motion and thus improves control robustness of prostheses, ortheses, and exoskeletons [2].

Activation of human muscles is accompanied by electrical stimulation of muscle fibers, followed by the mechanical response of the fibers contracting, leading to changes in muscle stiffness and shape. Electromyography (EMG) is a well-established method to detect human muscle activation, widely-exploited for wearables [3]–[5]. EMG relies either on non-invasive surface electrodes or on subcutaneous fine wire electrodes inserted into the muscle. In contrast, force myography (FMG) detects the mechanical phenomena related to muscle contraction rather than electrical effects. The detectable surface muscle pressure (SMP) correlates linearly with the intramuscular pressure (IMP) [6], suggesting that surface muscle pressure (SMP) can display both active and passive forces in the muscles [7], [8].
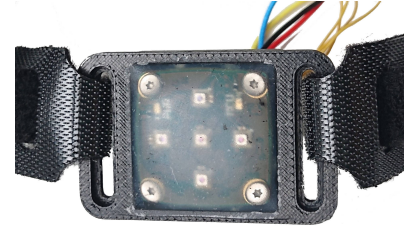
Fig. 1: Prototype of the proposed force myography sensor unit consisting of five barometric pressure sensors and an inertial measurement unit (IMU) covered by soft material.

In lower limb exoskeletons, surface electromyography (sEMG) and force myography (FMG) sensors are typically supplementary to foot switches, foot pressure insoles, and IMUs [4]. sEMG is useful for detecting gait phases since lower limb muscle activity occurs in a periodic manner during the gait cycle. However, sEMG sensors come with inherently higher complexity regarding data acquisition and post-processing, and the need for a direct skin-contact compared to FMG. Although the electrical activation of muscle fibers always precedes their mechanical contraction, the sEMG signal needs to be processed to control the prosthesis and this filtering inevitably leads to delays [9], [10]. The combination of sEMG and FMG sensors has shown to improve the accuracy of motion classification [3], [11]. Furthermore, both sensing modalities may even be joined in a co-located architecture, as successfully demonstrated in a hand gesture recognition task [5], [12]–[14].

In comparison, FMG-based signal processing is less prone to the condition of the skin contact and requires less signal filtering and post-processing. For instance, Islam et al. [15] showed that FMG outperforms surface electromyography (sEMG) in day-to-day motion detection because the data recorded from FMG sensors is more reliable and stable than sEMG. The accuracy of FMG-based gait event detection is comparable to that of pressure-sensitive insoles, gyroscopes, accelerometers, and electromyography, which are much more complex and expensive compared to FMG-based systems [16]. Additionally, FMG was shown to offer a better performance when compared to sEMG based threshold controllers [17], [18], in real-time control [19] and for joint angle estimation in both upper [20] and lower limbs [21], [22]. In muscle activity analysis of the thigh muscles, FMG showed considerable potential for detection and estimation of muscle activity and thus to determine muscle loads [23], [24].

FMG sensors may rely on different technologies, such as optical [25], capacitive [26], and resisitive transducing methods [27]. Among the above technologies, force sensing resistors (FSRs) are the most frequently used sensors for FMG since they are cost effective, easy to integrate, and thin. However, their nonlinear force-resistance response results in difficult calibration, and makes them prone to hysteresis [27]. Despite these drawbacks, their use is extensively investigated in various wearable applications [10], [15], [28]–[30]. Recently, barometer-based pressure sensors became smaller and accessible enough to be a promising alternative for use in FMG. For example, Dabling et al. [31] showed that barometer-based pressure sensors performed better in static drift and cyclic loading testing compared to FSRs, optical and capacitative sensors.

In our previous work [32], we explored the use of barometer-based sensors embedded in the fingertips of a soft prosthetic hand for haptic-based reactive grasping. This paper proposes to extend this barometric technology for interaction and muscle activity detection for exoskeleton devices. Namely, we propose a compact and low profile sensor unit based on barometric pressure sensor, as shown in Fig. 1. Our sensor unit robustly measures the normal forces resulting from the SMP of the muscles without the need of extensive calibration and post-processing. As expected, our sensor units are more invariant to the position on the muscle compared to sEMG electrodes. We validated the proposed sensor unit in a pilot study setup by comparing it with sEMG measurements of the *gastrocnemius lateralis* muscle with regard to its optimal position on the muscle and its inter-subject variability and variance.

The rest of the paper is organized as follows: Section II describes the design of the sensor unit and gives an overview about the experimental setup and trials used to evaluate the performance of the sensor unit. The results are presented in Section III and discussed in Section IV. Section V concludes the paper.

II. DESIGN AND EVALUATION METHODS

In this section, we describe the design of the barometer-based pressure sensor unit and the methods used to determine the force-pressure relationship, as well as the comparison of our FMG sensor unit with EMG sensors in human application.

A. Design

The sensor unit is designed to be comfortable to wear when integrated in an exoskeleton interface and provides information on the muscle stiffness, as well as the orientation of the sensor unit. It consists of five barometric pressure sensors, an IMU, and a microcontroller integrated on one single custom-made printed circuit board (PCB) and covered by soft material (see Fig. 1). The small square printed circuit board (PCB) allows the five barometric pressure sensors (BMP384, Bosch Sensortec) to be evenly distributed on the surface (see Fig. 2a) to ensure that all applied forces on the complete surface are accounted for. The IMU
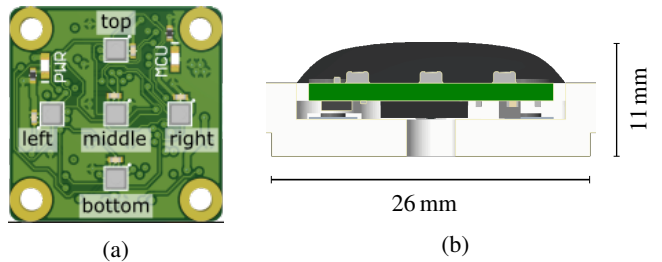

Fig. 2: Sensor unit design. (a) PCB with sensor identification. Pressure sensors are shown in the middle of each side (left, right, top, bottom) and in the center (middle). (b) Cross section of the sensor unit. Its silicone dome (black) is located above the pressure sensors (gray) and the PCB (green).

(BNO055, Bosch Sensortec) is located on the bottom side. The rigid housing of the PCB was manufactured from acrylonitrile styrene acrylate (ASA) using 3D-printing methods (fused deposition modeling). Making use of a 3D-printed mold (stereolithography) made of clear resin, the screwed-in PCB was completely cast in silicone of Shore hardness A (ShA) 13, leaving a dome-shaped soft cover over the pressure sensors (see Fig. 2b). The silicone hardness was empirically chosen based on prosthetic hand design results from previous work [33].

A microcontroller (STM32L5 series, STMicroelectronics) allows for communication with the barometric sensors via a serial peripheral interface (SPI). The pressure sensors transmit their signals with a sample frequency of 200 Hz. To distinguish the individual barometric pressure sensors for the experiments, they were named according to their position on the PCB, when oriented as shown in Fig. 2a. Each pressure sensor chip includes a temperature sensing element. Using the microcontroller and calibration data provided by Bosch Sensortec, the barometric pressure and temperature measurements are converted into MPa and °C respectively. The calibrated barometric sensor data is passed from the sensor unit via a universal asynchronous receiver-transmitter (UART) interface to a computer for processing and analysis.

B. Force-Pressure Characterization

We assess the performance of the sensor unit by conducting a series of experiments in which normal and shear forces are induced on a prototype sensor unit. The goal is to characterize the relationship between pressure and normal forces, as well as the detection of shear forces.

The experimental setup is shown in Fig. 3a and consists of a two-axis linear stage as used in our previous work [33]. Each of the axes is a precision linear stage (PT4808, MM Engineering GmbH) with a lead of 0.5 mm per revolution. Both axes are connected to stepper motors with 200 steps per revolution. A force/torque transducer (Mini 40, ATI Industrial Automation), used as reference force sensor, is mounted on the vertical shaft whereas the sensor is attached to the horizontal shaft, allowing the probe to apply well-defined normal forces onto the sensor unit. Moving the
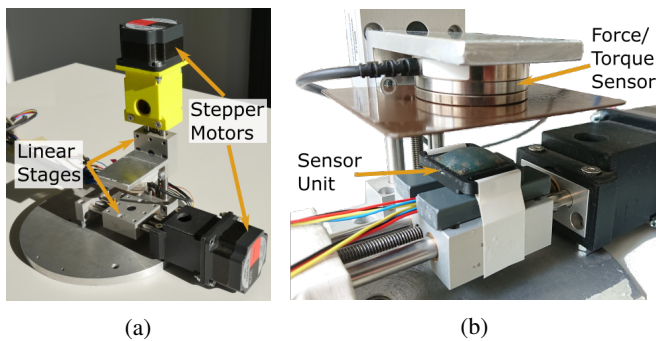
Fig. 3: Two-axis linear table for normal and shear force experiments. (a) General setup (adapted from [33]), (b) a close-up of the sensor attachment to the horizontal stage.
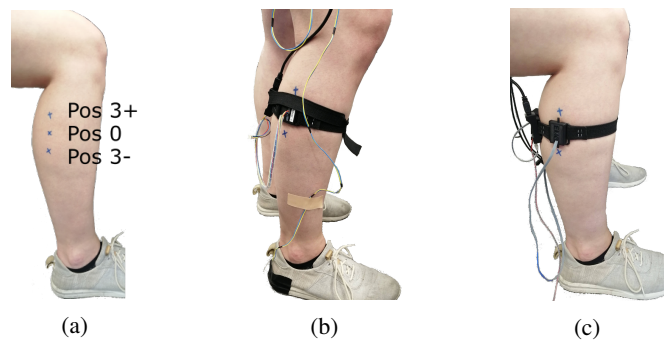

Fig. 4: Experimental setup on the human leg. (a) shows the three positions on the *gastrocnemius lateralis m.* (b) and (c) depict a sensor unit and an EMG electrode at position 0.

sensor horizontally while a normal force is applied evaluates the behavior when subjected to shear forces. Below the force/torque transducer, a rigid metal plate covers screw holes on the transducers surface and thus ensures an even distribution of the force onto the sensor (see Fig. 3b).

Synchronized recording of both force/torque transducer and pressure sensor data as well as control of linear stage movements is done using a Rasberry Pi via a Python script. Data was analyzed offline using MATLAB. Pressure data from the sensor unit was initialized under normal barometric air pressure before each experiment and all following data was calibrated with regard to this initial data.

For the normal force experiment the horizontal shaft in the aforementioned experimental setup was held in a fixed position while an increasing normal force was applied step-by-step to the sensor unit via a displacement of the vertical shaft. Similarly as in the literature [15], [21], [34], the maximum force of 10 N was set as limit. As soon as the saturation of the pressure sensors or the force limit was reached, the normal force was released and the horizontal shaft returned with the same resolution back into its initial position.

For the shear force experiments, we focused on the outer four sensors to investigate if those could detect the direction of the applied shear force. To evaluate the behavior regarding shear forces, a normal force of 3 N was continuously applied to the sensor unit. Afterwards an increasing shear force was applied step-by-step via a displacement of the horizontal shaft away from the stepper motor up to a maximum force of 1 N. In terms of the sensor identification (Fig. 2a), the sensor unit was moved from the side of its bottom sensor in the direction of its top sensor. After reaching its limit the shear force was decreased again and both shafts returned with the same velocity back into their initial position.

Both experiments were repeated with a sheet of 8 mm thick ethylene propylene diene monomer rubber (EPDM) attached to the bottom of the metal plate. According to the average stiffness of human soft tissue evaluated by Guitteny et al. [35], EPDM has a similar stiffness as human soft tissue and thus provides a possibility to simulate the pressure

sensor characteristics closer to a wearable application. Due to the shape of the silicone dome, a metal plate only applies forces at a contact point, whereas the human soft tissue will apply forces on the complete surface. This is expected to influence the behavior of the sensor and thus its force-pressure relation [36].

C. EMG-FMG Characterization

For the EMG-FMG characterization, walking experiments were conducted in a pilot study with four participants. Informed consent was obtained from all participants involved in the study. The experimental setup consisted of an EMG electrode (13E200, Ottobock SE & Co. KGaA) with an integrated amplifier and the presented pressure sensors unit. The sensors were placed anatomically to measure activity from the *gastrocnemius lateralis m.* at the rear of the shank.

Both sensors were positioned at three different positions along the *gastrocnemius lateralis m.* at a distance of 3 cm (Figs. 4a and 4b). The position (Pos. 0) was determined based on EMG placement recommendations from SENIAM [37] combined with the strongest EMG signal along the muscle according to real-time feedback from the sensor. The other two positions (Pos. 3+ and Pos. 3- were chosen 3 cm upwards and downwards of the optimal position along the muscle. After donning the setup the participants had a few minutes to get used to all sensors and cables while walking freely. For each experiment the participants were than asked to stand upright in a relaxed way for approximately 10 s before walking about 45 strides in a straight line at a speed rate of about 100 strides per minute.

For the pressure sensor unit, the mean signal of all five barometric sensors was calculated. The EMG electrode was adjusted to the maximum amplification level. All sensor data was calibrated using the data from the standing phase. Detection of each heel strike to determine each full gait cycle was analyzed based on a miniature switch (D2F-L, OMRON Corporation) attached to the right heel (sensorized leg). The full data was reduced to 36 strides within the walking data to ensure the participant has adjusted to the speed rate and reached a consistent stride length. Analysis of the data was conducted in MATLAB.
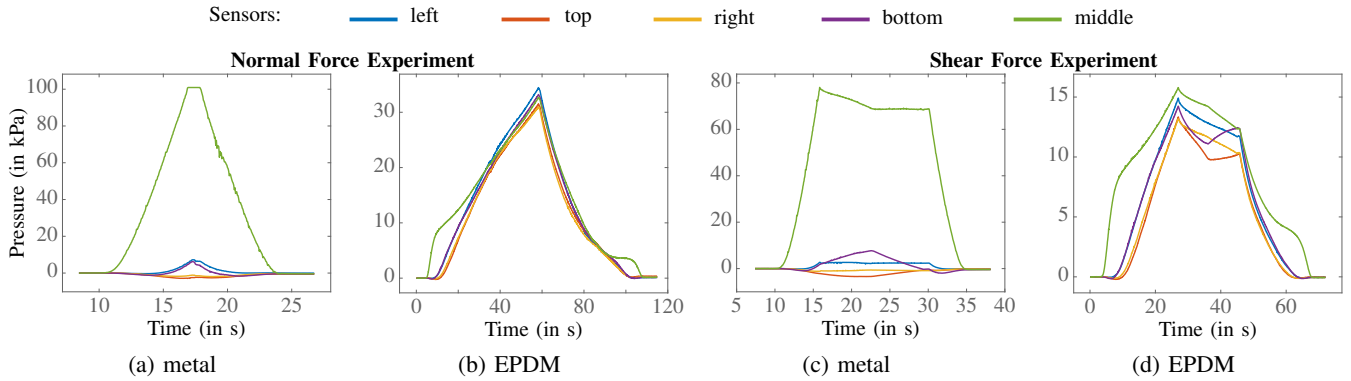
Fig. 5: Normal and shear force experiments of the barometric pressure sensors. Signals are shown for each single pressure sensor on the PCB according to the sensor identification.

III. RESULTS

In this section, we describe the results of the sensor unit characterization based on the methods and experiments described above.

A. Force-Pressure Characterization

According to its data sheet, each barometric pressure sensor saturates by design at an absolute pressure of 125 kPa. Covered by a silicone layer, calibrated without load and subjected to a normal force, this corresponds to about 5 N when applied by a plain metal sheet (see Fig. 5a). If an 8 mm EPDM layer is added to replicate human soft tissue, the applicable normal force exceeds the measured maximum normal force of 10 N (see Fig. 5b). The EPDM layer is completely covering the silicone dome and all sensors within the unit report a change in pressure instead of only the middle sensor in case of the stiff metal plate in the first experiment.

Fig. 6 compares the normal force measurements to the two material configurations of the experimental setup using the mean signal of all five barometric pressure sensors within one sensor unit. Whereas the force-pressure relation shows a very low hysteresis between the measured pressure signals
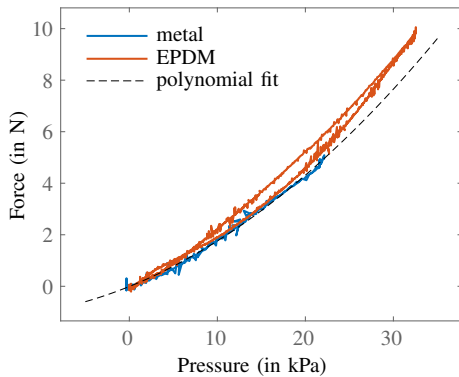

Fig. 6: Force-pressure relation: mean signal of all five barometric sensors within the sensor unit of both purely the metal and the attached 8 mm EPDM layer, as well as the polynomial model for the former.

and the applied force in the plain metal configuration, it is slightly more prominent with the additional foam. Fitting a polynomial model to the measured force F and pressure P data in the plain metal configuration results in

$$F = 0.003928 \cdot P^2 + 0.1375 \cdot P - 0.007911$$

with a coefficient of determination R^2 of 99.63 %.

When subjected to shear forces, the data from the experiments with the plain metal sheet displays increased and decreased pressure in the bottom and top barometric sensor, respectively (see Fig. 5c). Adding a layer of EPDM also leads to a visible change in the behavior of the top and bottom barometric pressure sensor, however, both sensors in the corresponding plane show a decrease when subjected to shear forces.

B. EMG-FMG Characterization

Figs. 7a and 7b display the signal mean of the electric potential and pressure of 36 strides by one participant measured at the three different positions along the muscle during the gait cycle. The results suggests that on the *gastrocnemius lateralis m.* the most distinct signal of the EMG electrode can be retrieved from Pos. 0 while the surface pressure can be measured at different positions on the muscle with a similarly strong signal.

Comparing the trajectory of the EMG signal and the measured SMP of all four participants in Figs. 7c and 7d, both display a low inter-subject variability if donned in Pos. 0. The variance of the pressure appears lower during the stance phase compared to the swing phase. If donned at the two other positions, the EMG shows a high variance between participants, whereas the inter-subject variability of the pressure signal remains similar.

Fig. 8 additionally shows that in both Pos. 3+ and Pos. 3- the electric potential displays a high standard deviation and deviates strongly from Pos. 0. The pressure signal shows a lower variance through the change of the position. Additionally, the deviation from the trajectory at its optimal position is less obvious than the EMG signal.
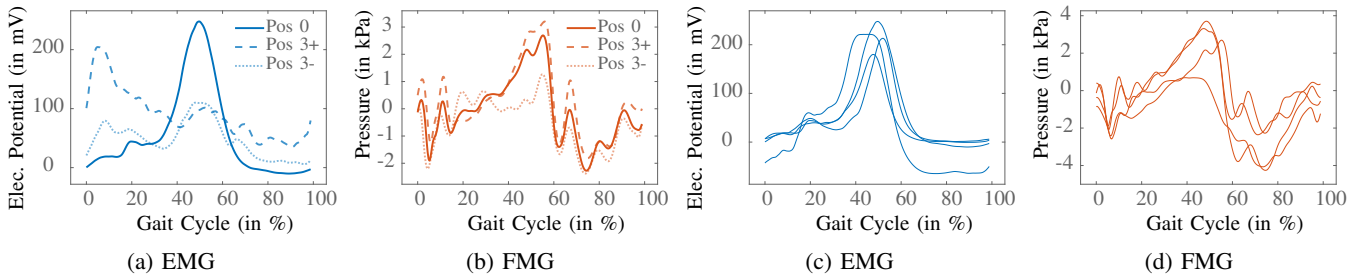
Fig. 7: Comparison of the mean signal of both the EMG (blue) and the FMG (orange) signal of the *gastrocnemius lateralis m.* generalized from 36 strides of (a)-(b) one participant at all positions and (c)-(d) all participants at position 0.

IV. DISCUSSION

This paper presents a concept and implementation of a sensor unit consisting of five barometric pressure sensors encased in soft silicone. In this section, we discuss the results of each characterization in a broader context and with regard to related work.

A. Force-Pressure Characterization

The barometric pressure sensors within the sensor unit offer a suitable performance for low forces and show a close to linear force-pressure relationship with a comparatively low hysteresis, the latter being presumably only a result of the silicone dome with its slightly visco-elastic properties. In its application it will also be influenced by the thickness and characteristic of the soft tissue (here simulated by EPDM foam) between the muscle and the sensor.

The comparison of the mean value of all five barometric pressure sensors in Fig. 6 shows, that not only does the EPDM apply pressure to all five sensors, but it also evenly distributes the pressure to all sensors. This allows for an increased total force range of more than 10 N and a robustness to varying stiffness in the human soft tissue. Similar findings have been reported by [36]. The applicable force range also aligns with previous findings on FSR sensors in literature [15], [21], [34]. However, the pressure sensor unit displays more linear behavior regarding the applied force in relation to the measured pressure signal compared to the characteristic of FSR sensors described in [27]. In comparison to FSR sensors, this makes the barometer-based pressure sensor unit sensitive to small forces.

In the experiments, we evaluated whether shear forces could also be tracked by an array of barometric pressure sensors under a silicone dome. The results in Figs. 5c and 5d reveal that in a configuration where only a rigid metal plate induces shear forces, those shear forces and their direction can be detected. However, in a setting closer to the human soft tissue (EPDM) only the fact that shear forces occur can be detected, but not their direction and magnitude. Solely the plane in which shear forces are applied can be recognized from the changing trajectory of the barometric pressure sensors within that plane. Further designs could include the Hall-effect based sensors presented in [38] or a different arrangement of the barometric pressure sensors to achieve shear force detection regarding direction and dynamic. In its target application, i.e., a lower limb exoskeleton interface, shear force detection allows the evaluation of the influence of misalignment or slip of an interface shell on the sensor signals. At the same time this would give information to evaluate the design of the exoskeleton regarding misalignment which strongly contributes to the comfort and acceptance of an exoskeleton.

One limitation of our experiments was the application of low shear forces with regard to the applied normal force (approximately a maximum of 30 % to 35 % for metal and about 40 % to 50 % for the EPDM configuration. The restricting factor was the point at which the kinetic friction replaces the static friction between the silicone surface and the opposing metal or EPDM surface. Moreover, only slow motion loading tests were evaluated. In the future, additional cyclic loading tests could provide a better understanding of
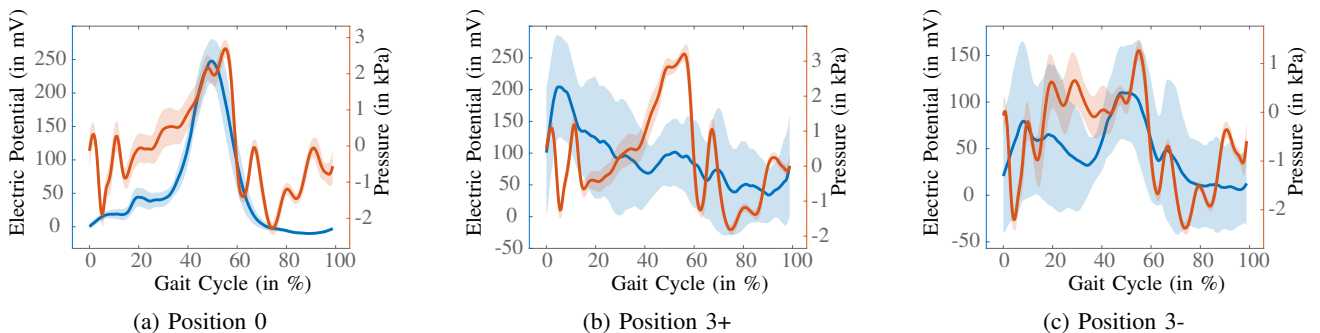

Fig. 8: Mean and standard deviation of the EMG (blue) and FMG (orange) signal of the *gastrocnemius lateralis m.* of each position generalized from 36 strides of one participant.

the characteristics of the sensor unit for its integration in wearable robots and usage in dynamic settings.

B. EMG-FMG Characterization

The pilot study explored the measurement of mechanical and electrical muscle activation signals (FMG and EMG respectively) on the *gastrocnemius lateralis m.* during ground-level walking. An offset was calculated from the data while standing which allowed for a better quantification of the muscle activity. Each sensor successfully measured the respective activity of the muscle and the collected data allowed for a preliminary evaluation of the characteristics of the SMP measured by the pressure sensor unit in comparison to EMG.

A key investigation point of this pilot study was to determine the robustness of the pressure sensor unit to its placement on the muscle. As expected, the electrical muscle activation can be optimally measured at 1/3 of the line between head of the fibula and the heel [37], here Pos. 0. However, the mechanical muscle response, the SMP, can be measured in a wider range along the muscle while still providing a distinct trajectory with low variance and only a small difference in magnitude. Any influence of co-contractions of neighboring muscles cannot be excluded in this dynamic setting, but appear to be consistent independent on the position on the sensor. Thus the pressure sensor unit appears to be more robust and invariant to its positioning on the muscle offering a simple integration into an exoskeleton shell and thus an easier donning for the user.

Another investigation point of the pilot study was concerned with the inter-subject variability in sensor signals whilst recording the muscle activation via EMG electrodes or the muscle response via our pressure sensor unit. The resulting activation-response delay is reflected in Figs. 7 and 8, similar as it has been observed for the *quadriceps* by [23]. Independent of the position of the sensor, the peak of the SMP appears slightly delayed to the electrical activation and persists slightly longer eventually including a second peak. In contrast to the electric potential sent to activate the muscle, the muscular reaction is influenced by genetics and preconditioning variances including the soft tissue between the muscle and the pressure sensor unit [39], [40]. However, the experiments suggest that the inter-subject variability with our presented pressure sensor units is lower than expected and shows consistency in shape and amplitude of the sensor signals during ground-level walking, particularly during the stance phase.

Limitations of our walking trials include unknown influences due to a change in circumference of the lower leg and oscillations resulting from movement of the sensor with respect to the skin. Co-contractions of other muscles around the leg can lead to circumferential changes which could potentially be interpreted as muscles forces by the sensor unit. An elastic band included into the design of the experimental sensor attachment aimed to minimize those influences. At the same time, this allows the sensor unit to move more freely with respect to the skin if impacted by the heel strike, which might lead to the oscillations in the beginning of the gait cycle in Figs. 7b and 7d. It is expected that this should improve when the sensor is integrated into the shell of an exoskeleton.

The effect of temperature changes on the behavior of the sensor is not explored in this work. The barometric measurement technique in the integrated sensors are based on temperature changes. If the temperature inside the silicone dome rises, the measured value may change. To account for this, the sensor unit was initialized roughly 10 min after donning, so that the silicone already adapted to the user's body temperature. Still, high exertion could potentially cause the user to have higher skin temperatures. However, the walking trials in our study were short and relaxed to reduce such influences.

V. CONCLUSION

In this paper, we present a a wearable, compact and low profile sensor unit based on barometric pressure sensors for robust interaction and muscle activity detection in wearable applications such as exoskeletons, but also motion analysis. A prototype was experimentally evaluated to explore both its sensor characteristics and its performance based on data collected in a pilot study. Results showed that the pressure sensor unit can successfully measure a suitable range of normal forces with an almost linear characteristic and provide a promising method to measure muscle activity during dynamic motion with a rather low inter-subject variability. Further research will focus on the relation between the measurement systems for EMG and FMG in more detail, focusing on muscle activity under loading strain in a setup minimizing any influence of co-contraction. The presented results will be validated in a larger scale and enhanced by further activities of daily living. The invariance to positioning the sensor unit on the muscle is an important property in its target application of an exoskeleton interface shell, allowing for a robust estimation of the muscle activity. This approach could potentially be used as a basis of a multi-level control approach for assistive exoskeletons, providing biofeedback enabling the estimation of muscle state even above clothing during activities of daily living.

REFERENCES

[1] A. Rodríguez-Fernández, J. Lobo-Prat, and J. M. Font-Llagunes, "Systematic review on wearable lower-limb exoskeletons for gait training in neuromuscular impairments," *Journal of NeuroEngineering and Rehabilitation*, vol. 18, no. 1, p. 22, Dec. 2021.

[2] T. Wang, B. Zhang, C. Liu, T. Liu, Y. Han, S. Wang, J. P. Ferreira, W. Dong, and X. Zhang, "A Review on the Rehabilitation Exoskeletons for the Lower Limbs of the Elderly and the Disabled," *Electronics*, vol. 11, no. 3, p. 388, Jan. 2022.

[3] C. D. Joshi, U. Lahiri, and N. V. Thakor, "Classification of gait phases from lower limb emg: Application to exoskeleton orthosis," in *IEEE Point-of-Care Healthcare Technologies (PHT)*, Jan 2013, pp. 228–231.

[4] J. Taborri, E. Palermo, S. Rossi, and P. Cappa, "Gait partitioning methods: A systematic review," *Sensors*, vol. 16, no. 1, 2016.

[5] S. Jiang, P. Kang, X. Song, B. Lo, and P. B. Shull, "Emerging Wearable Interfaces and Algorithms for Hand Gesture Recognition: A Survey," *IEEE Reviews in Biomedical Engineering*, pp. 1–1, 2021.

[6] J. R. Cram, G. S. Kasman, and J. Holtz, *Introduction to surface electromyography*. Aspen publishers, 1998.

[7] M. K. MacLean and D. P. Ferris, "Human muscle activity and lower limb biomechanics of overground walking at varying levels of simulated reduced gravity and gait speeds," *PLOS ONE*, vol. 16, no. 7, pp. 1–23, 07 2021.

[8] S. Hwang, H.-M. Lee, R.-J. Cherng, and J.-J. J. Chen, "Electromyographic analysis of locomotion for healthy and hemiparetic subjects—study of performance variability and rail effect on treadmill," *Gait & Posture*, vol. 18, no. 1, pp. 1–12, 2003.

[9] D. Esposito, G. D. Gargiulo, N. Parajuli, G. Cesarelli, E. Andreozzi, and P. Bifulco, "Measurement of muscle contraction timing for prosthesis control: a comparison between electromyography and forcemyography," in *IEEE International Symposium on Medical Measurements and Applications (MeMeA)*, Jun. 2020, pp. 1–6.

[10] D. Esposito, E. Andreozzi, A. Fratini, G. Gargiulo, S. Savino, V. Niola, and P. Bifulco, "A Piezoresistive Sensor to Measure Muscle Contraction and Mechanomyography," *Sensors*, vol. 18, no. 8, p. 2553, Aug. 2018.

[11] I. Patzer and T. Asfour, "Minimal sensor setup in lower limb exoskeletons for motion classification based on multi-modal sensor data," in *IEEE/RSJ International Conference on Intelligent Robots and Systems (IROS)*. Macau, China: IEEE, November 2019, pp. 8158–8164.

[12] S. Jiang, Q. Gao, H. Liu, and P. B. Shull, "A novel, co-located EMG-FMG-sensing wearable armband for hand gesture recognition," *Sensors and Actuators A: Physical*, p. 111738, 2020.

[13] P. B. Shull, S. Jiang, Y. Zhu, and X. Zhu, "Hand Gesture Recognition and Finger Angle Estimation via Wrist-Worn Modified Barometric Pressure Sensing," *IEEE Transactions on Neural Systems and Rehabilitation Engineering*, vol. 27, no. 4, pp. 724–732, Apr. 2019.

[14] M. Connan, E. Ruiz Ramírez, B. Vodermayer, and C. Castellini, "Assessment of a Wearable Force- and Electromyography Device and Comparison of the Related Signals for Myocontrol," *Frontiers in Neurorobotics*, vol. 10, 2016.

[15] M. R. U. Islam and S. Bai, "Effective Multi-Mode Grasping Assistance Control of a Soft Hand Exoskeleton Using Force Myography," *Frontiers in Robotics and AI*, vol. 7, p. 139, 2020.

[16] A. K. Godiyal, H. K. Verma, N. Khanna, and D. Joshi, "A Force Myography-Based System for Gait Event Detection in Overground and Ramp Walking," *IEEE Transactions on Instrumentation and Measurement*, vol. 67, no. 10, pp. 2314–2323, Oct. 2018.

[17] X. Jiang, L.-K. Merhi, Z. G. Xiao, and C. Menon, "Exploration of Force Myography and surface Electromyography in hand gesture classification," *Medical Engineering & Physics*, vol. 41, pp. 63–73, Mar. 2017.

[18] N. Jaquier, M. Connan, C. Castellini, and S. Calinon, "Combining Electromyography and Tactile Myography to Improve Hand and Wrist Activity Detection in Prostheses," *Technologies*, vol. 5, no. 4, p. 64, Dec. 2017.

[19] A. Belyea, K. Englehart, and E. Scheme, "FMG Versus EMG: A Comparison of Usability for Real-Time Pattern Recognition Based Control," *IEEE Transactions on Biomedical Engineering*, vol. 66, no. 11, pp. 3098–3104, Nov. 2019.

[20] M. R. U. Islam, K. Xu, and S. Bai, "Position Sensing and Control with FMG Sensors for Exoskeleton Physical Assistance," in *Wearable Robotics: Challenges and Trends*, ser. Biosystems & Biorobotics, M. C. Carrozza, S. Micera, and J. L. Pons, Eds. Springer International Publishing, 2019, pp. 3–7.

[21] X. Jiang, H. T. Chu, Z. G. Xiao, L.-K. Merhi, and C. Menon, "Ankle positions classification using force myography: An exploratory investigation," in *IEEE Healthcare Innovation Point-Of-Care Technologies Conference (HI-POCT)*, Nov. 2016, pp. 29–32.

[22] A. Kumar, A. K. Godiyal, P. Joshi, and D. Joshi, "A New Force Myography-Based Approach for Continuous Estimation of Knee Joint Angle in Lower Limb Amputees and Able-Bodied Subjects," *IEEE Journal of Biomedical and Health Informatics*, vol. 25, no. 3, pp. 701–710, Mar. 2021.

[23] D. A. Yungher, M. T. Wininger, J. B. Barr, W. Craelius, and A. J. Threlkeld, "Surface muscle pressure as a measure of active and passive behavior of muscles during gait," *Medical Engineering & Physics*, vol. 33, no. 4, pp. 464–471, May 2011.

[24] A. Belbasis, F. K. Fuss, and J. Sidhu, "Muscle Activity Analysis with a Smart Compression Garment," *Procedia Engineering*, vol. 112, pp. 163–168, Jan. 2015.

[25] A. Ribas Neto, J. Fajardo, W. H. A. da Silva, M. K. Gomes, M. C. F. de Castro, E. Fujiwara, and E. Rohmer, "Design of Tendon-Actuated Robotic Glove Integrated with Optical Fiber Force Myography Sensor," *Automation*, vol. 2, no. 3, pp. 187–201, Sep. 2021.

[26] S. Crea, S. Manca, A. Parri, E. Zheng, J. Mai, R. M. Lova, N. Vitiello, and Q. Wang, "Controlling a Robotic Hip Exoskeleton With Noncontact Capacitive Sensors," *IEEE/ASME Transactions on Mechatronics*, vol. 24, no. 5, pp. 2227–2235, Oct. 2019.

[27] J. S. Schofield, K. R. Evans, J. S. Hebert, P. D. Marasco, and J. P. Carey, "The effect of biomechanical variables on force sensitive resistor error: Implications for calibration and improved accuracy," *Journal of Biomechanics*, vol. 49, no. 5, pp. 786–792, Mar. 2016.

[28] H. Choi, K. Seo, S. Hyung, Y. Shim, and S.-C. Lim, "Compact hip-force sensor for a gait-assistance exoskeleton system," *Sensors*, vol. 18, no. 2, 2018.

[29] M. R. U. Islam, A. Waris, E. N. Kamavuako, and S. Bai, "A comparative study of motion detection with FMG and sEMG methods for assistive applications," *Journal of Rehabilitation and Assistive Technologies Engineering*, vol. 7, pp. 1–11, Jan. 2020.

[30] A. K. Godiyal and D. Joshi, "Optimal Force Myography Placement For Maximizing Locomotion Classification Accuracy in Transfemoral Amputees: A Pilot Study," *IEEE Journal of Biomedical and Health Informatics*, vol. 25, no. 4, pp. 959–968, Apr. 2021.

[31] J. G. Dabling, A. Filatov, and J. W. Wheeler, "Static and cyclic performance evaluation of sensors for human interface pressure measurement," in *Annual International Conference of the IEEE Engineering in Medicine and Biology Society*, Aug 2012, pp. 162–165.

[32] P. Weiner, F. Hundhausen, R. Grimm, and T. Asfour, "Detecting grasp phases and adaption of object-hand interaction forces of a soft humanoid hand based on tactile feedback," in *IEEE/RSJ International Conference on Intelligent Robots and Systems (IROS)*, Prague, Czech Republic, September 2021, pp. 3956–3963.

[33] P. Weiner, C. Neef, Y. Shibata, Y. Nakamura, and T. Asfour, "An embedded, multi-modal sensor system for scalable robotic and prosthetic hand fingers," *Sensors*, vol. 20, no. 1, pp. 108–121, 2019.

[34] A. K. Godiyal, M. Mondal, S. D. Joshi, and D. Joshi, "Force Myography Based Novel Strategy for Locomotion Classification," *IEEE Transactions on Human-Machine Systems*, vol. 48, no. 6, pp. 648–657, Dec. 2018.

[35] S. Guitteny, Y. Lafon, V. Bonnet, R. Aissaoui, and R. Dumas, "Dynamic estimation of soft tissue stiffness for use in modeling socket, orthosis or exoskeleton interfaces with lower limb segments," *Journal of Biomechanics*, vol. 134, p. 110987, Mar. 2022.

[36] K. Langlois, E. Roels, G. Van De Velde, C. Espadinha, C. Van Vlerken, T. Verstraten, B. Vanderborght, and D. Lefeber, "Integration of 3D Printed Flexible Pressure Sensors into Physical Interfaces for Wearable Robots," *Sensors*, vol. 21, no. 6, p. 2157, Jan. 2021.

[37] H. J. Hermens, B. Freriks, R. Merletti, D. Stegeman, J. Blok, G. Rau, C. Disselhorst-Klug, and G. Hägg. (1999) Seniam. [Online]. Available: http://seniam.org/

[38] T. P. Tomo, S. Somlor, A. Schmitz, L. Jamone, W. Huang, H. Kristanto, and S. Sugano, "Design and Characterization of a Three-Axis Hall Effect-Based Soft Skin Sensor," *Sensors*, vol. 16, no. 4, p. 491, Apr. 2016.

[39] C. J. De Luca, "The use of surface electromyography in biomechanics," *Journal of Applied Biomechanics*, vol. 13, no. 2, pp. 135 – 163.

[40] J. Z. Liu, R. W. Brown, and G. H. Yue, "A Dynamical Model of Muscle Activation, Fatigue, and Recovery," *Biophysical Journal*, vol. 82, no. 5, pp. 2344–2359.